ELSEVIER

NeuroImage

www.elsevier.com/locate/ynimg
NeuroImage 32 (2006) 9 – 15

Caffeine reduces the initial dip in the visual BOLD response at 3 T

Yashar Behzadi[a,b] and Thomas T. Liu[a,*]

[a]*Center for Functional Magnetic Resonance Imaging and Department of Radiology, University of California San Diego, 9500 Gilman Drive, La Jolla, MC 0677, CA 92093-0677, USA*
[b]*Department of Bioengineering, University of California San Diego, La Jolla, CA 92093-0677, USA*

Received 13 January 2006; revised 22 February 2006; accepted 7 March 2006
Available online 25 April 2006

Localized changes in oxygen consumption related to increased neural activity can result in a small and transient "initial dip" of the blood oxygenation level-dependent (BOLD) signal used in functional magnetic resonance imaging (fMRI). The initial dip has been of great interest to the fMRI community because it may provide a more accurate and localized measure of neural activity than the conventional BOLD signal increase. Although potentially useful as a technique for human brain mapping, the initial dip is not always detected and has been a source of some controversy. In this study, the BOLD response to a 4-s long visual stimulus was measured with a 3-T MRI system in 5 healthy volunteers both before and immediately after a 200-mg oral caffeine dose. The caffeine dose significantly ($P < 0.001$) reduced or eliminated the initial dip in all subjects. These findings suggest that caffeine usage may be a key factor in the detection of the initial dip in human fMRI studies.

Introduction

The blood oxygenation level-dependent signal (BOLD) used in most functional magnetic resonance imaging (fMRI) studies reflects local changes in deoxyhemoglobin (dHb). With increased neural activity, there are increases in both the rate of oxygen metabolism ($CMRO_2$) and the delivery of oxygen via cerebral blood flow (CBF). In most cases, the increase in oxygen delivery eventually exceeds the rate of oxygen consumption, leading to a prolonged decrease in dHb and an increase in the BOLD response (Buxton et al., 1998). This signal increase, referred to as the positive BOLD response, is the basis for most fMRI applications. However, a number of optical imaging and functional magnetic resonance imaging (fMRI) studies have shown that, in the first few seconds following the onset of increased neural activity, $CMRO_2$ may increase more quickly than CBF, leading to an initial transient increase in dHb and an associated "initial dip" in the BOLD signal (Ernst and Hennig, 1994; Menon et al., 1995; Malonek and Grinvald, 1996; Hu et al., 1997; Thompson et al., 2004). In addition, it has been shown that the initial dip is better localized to areas of neural activity (e.g., cortical columns), as compared to the more diffuse positive BOLD response (Duong et al., 2000; Yacoub et al., 2001; Kim et al., 2000; Yacoub and Hu, 2001). These observations are consistent with a view in which the early portion of the BOLD signal reflects changes in dHb that are primarily localized to the microvasculature, whereas the later part of the BOLD signal reflects dHb changes in both the microvasculature and the macrovasculature, due to the draining of dHb into larger vessels (Duong et al., 2000; Fukuda et al., 2006; Yacoub et al., 2001).

Although the initial dip has been observed in a number of human and animal studies (Ernst and Hennig, 1994; Malonek and Grinvald, 1996; Hu et al., 1997; Vanzetta and Grinvald, 1999; Duong et al., 2000; Kim et al., 2000; Yacoub and Hu, 2001; Yacoub et al., 2001), some animal studies have found no evidence for an initial dip (Mandeville et al., 1999; Marota et al., 1999; Silva et al., 2000; Lindauer et al., 2001). It has been suggested that differences in imaging methodology, brain regions, animal species, and anesthesia are responsible for the conflicting observations in animal studies (Buxton, 2001; Ances, 2004). One human fMRI study suggested that the initial dip may be an experimental artifact that arises when stimuli are too closely spaced in time (Fransson et al., 1998), but a subsequent study found an initial dip even with wider spacings (Yacoub et al., 1999). While there do not appear to be additional human fMRI studies that explicitly focus on the absence of the initial dip, there are many studies of the dynamics of the BOLD response that either do not find or simply do not mention the initial dip. For example, the initial dip was not observed in studies examining the effects of carbon dioxide on the BOLD response (Kemna and Posse, 2001; Cohen et al., 2002). Cohen et al. attributed the lack of detection to differences in experimental methodology, which can be an important factor given the relatively small amplitude of the initial dip.

In addition to methodological differences, variations in the baseline vascular state due to factors such as pharmacological

* Corresponding author. Fax: +1 858 822 0605.
E-mail address: ttliu@ucsd.edu (T.T. Liu).
Available online on ScienceDirect (www.sciencedirect.com).

1053-8119/$ - see front matter © 2006 Elsevier Inc. All rights reserved.
doi:10.1016/j.neuroimage.2006.03.005

agents, disease, and age have been shown to alter the dynamics of the BOLD response and may therefore affect the detection of the initial dip in humans (D'Esposito et al., 2003). As an example, the carbon dioxide studies mentioned above found that vasodilation caused by hypercapnia significantly slowed down the dynamics of the BOLD response, while vasoconstriction caused by hypocapnia led to a quickening of the response. In a recent study using a 4-T MRI system, we showed that caffeine, a known vasoconstrictor, led to a quickening of the visual BOLD response in a manner similar to that observed with hypocapnia (Liu et al., 2004). Due to technical considerations (e.g., scanner instabilities), the initial dip was not easily detected in that study. In the present study, performed on a 3-T MRI system, we demonstrate robust detection of the initial dip and show that a 200 mg caffeine dose can significantly reduce the initial dip.

Methods

Experimental protocol

Five healthy subjects (ages 23 to 39) participated in the study after giving informed consent. Each subject refrained from ingesting any food or drink containing caffeine for at least 12 h prior to the experiment. The estimated daily caffeine usage of the subjects based on self-reports of coffee, tea, and caffeinated soda consumption is summarized in Table 1. The assumed caffeine contents for an 8-oz coffee, tea, and soda were 100 mg, 40 mg, and 20 mg, respectively (Fredholm et al., 1999). Each experiment lasted approximately 3 h and consisted of a 1-h pre-dose imaging session followed by a 1-h post-dose session. In addition to the actual time spent on imaging, the length of each session included time for preparation (e.g., ensuring that physiological monitoring equipment was working properly), parameter set-up and execution of pre-scan routines (as necessary), and instruction of the subject prior to each scan. Between sessions, the subject ingested an over-the-counter tablet containing 200 mg of caffeine and rested outside the scanner for approximately 30 min. The first functional run began approximately 45 min post-ingestion. This interval was chosen based on studies showing that the absorption of caffeine from the gastrointestinal tract reaches 99% about 45 min after ingestion, with a half-life of 2.5 to 4.5 h (Fredholm et al., 1999).

During both the pre-dose and post-dose imaging sessions, each subject viewed two repeats of a periodic single trial visual stimulus consisting of a 20-s initial "off" period followed by 5 cycles of a 4-s "on" period and a 40-s "off" period. During the "on" periods, a full-field, full contrast radial 8-Hz flickering checkerboard was displayed, while the "off" periods consisted of a gray background of luminance equal to the average luminance of the "on" period. Three of the five subjects viewed two additional repeats of the periodic single trial design. As described below, these were acquired with a smaller imaging slice thickness than the first two repeats. In addition, a resting-state scan, during which the subject was presented with the "off" condition for 3 min, was performed and used to characterize the resting CBF level.

Imaging protocol

Imaging data were collected on a GE Signa Excite 3 Tesla whole body system with a body transmit coil and an eight channel receive coil. Laser alignment was used to landmark the subject and minimize differences in head position between sessions. During the resting-state scan, data were acquired with a PICORE QUIPPS II (Wong et al., 1998) arterial spin labeling (ASL) sequence (TR = 2 s, TI1/TI2 = 600/1500 ms, 10-cm tag thickness, and a 1-cm tag-slice gap) with a dual echo spiral readout (TE1/TE2 = 9.1/30 ms, FOV = 24 cm, 64 × 64 matrix, and a flip angle = 90°). Small bipolar crusher gradients were included to remove signal from large vessels (b = 2 s/mm^2). Three oblique axial 8-mm slices were prescribed about the calcarine sulcus for this ASL run. During the periodic single trial runs, BOLD-weighted images were acquired with a spiral readout (TE = 25 ms, TR = 500 ms, FOV = 24 cm, 64 × 64 matrix, and a flip angle of 45°). In all five subjects, these BOLD runs used the same slice prescription as the ASL runs (e.g., three 8-mm slices). The choice of the 8-mm slice thickness reflects the fact that the experiments on two of the subjects (labeled as Subjects 4 and 5 in Results) were not originally intended to examine the initial dip. To determine whether there was an effect of the large slice thickness, the experiments in the three remaining subjects (labeled 1 to 3 in Results) included two additional BOLD-weighted runs using the periodic single trial design and acquired with six oblique 4-mm slices covering the same volume as the three 8-mm slices. For all periodic single trials acquired at either slice thickness, 480 volumes at a TR of 500 ms were acquired.

A high-resolution structural scan was acquired with a magnetization prepared 3D fast spoiled gradient acquisition in the steady-state (FSPGR) sequence (TI 450 ms, TR 7.9 ms, TE 3.1 ms, 12° flip angle, FOV 25 × 25 × 16 cm, matrix 256 × 256 × 124). In addition, a cerebrospinal fluid (CSF) reference scan and a minimum contrast scan were acquired for use in CBF quantification. The CSF scan consisted of a single-echo, single repetition scan acquired at full relaxation and echo time equal to 9.1 ms, while the minimum contrast scan was acquired at TR = 2 s and TE = 11 ms. Both scans used the same in-plane parameters as the ASL scans, but the number of slices was increased to cover the lateral ventricles.

Table 1
Pre-dose and post-dose baseline CBF values shown as mean (standard deviation)

Subject	Estimated daily caffeine usage (mg)	Pre-dose baseline CBF ml/(100 g min)	Post-dose baseline CBF ml/(100 g min)	Paired t test P Value
1	200	53.4 (28.1)	33.5 (16.1)	3.9 e−18
2	<50	57.6 (23.3)	35.1 (16.8)	2.4 e−20
3	200	55.4 (22.6)	38.9 (20.2)	1.7 e−11
4	<50	73.1 (14.0)	35.8 (15.9)	1.0 e−19
5	250	88.2 (25.2)	47.4 (21.8)	1.8 e−19

Mean and standard deviation were computed across voxels in each subject's respective ROI_{dip}. For each subject, significance was computed with a paired t test (two-sided).

Cardiac pulse and respiratory effort data were monitored using a pulse oximeter (InVivo) and a respiratory effort transducer (BIOPAC), respectively. The pulse oximeter was placed on the subject's right index finger, and the respiratory effort belt was placed around the subject's abdomen. Physiological data were sampled at 40 samples per second using a multi-channel data acquisition board (National Instruments).

Data analysis

All images were coregistered using AFNI software (Cox, 1996). The structural scan from each post-dose session was aligned to the structural scan of its respective pre-dose session, and the rotation and shift matrix used for this alignment was then applied to the post-dose BOLD and ASL images. An image-based retrospective correction method RETROICOR (Glover et al., 2000; Restom et al., 2004) was used to reduce physiological noise due to cardiac and respiratory fluctuations. For each subject, a mean ASL image was formed from the average difference of the control and tag images from the resting-state scan data. This mean ASL image was then corrected for coil inhomogeneities using the minimum contrast image (Wang et al., 2005) and converted to physiological units using the CSF image as a reference signal (Chalela et al., 2000).

For each slice thickness, average BOLD time series were formed from the data (after physiological noise correction) for the two runs acquired at that thickness. All subsequent analyses were performed separately for the average BOLD time series. Correlation analysis was performed using a positive BOLD reference function formed by convolving the periodic single trial stimulus pattern with a gamma density function of the form $h(t) = (\tau n!)^{-1}((t - \Delta t)/\tau)\exp(-(t - \Delta t)/\tau)$ for $t \geq \Delta t$ and 0 otherwise, with $\tau = 1.2$, $n = 3$ and $\Delta t = 1$. A constant term and linear trend term were used as nuisance terms in the correlation analysis.

Functional regions of interest (ROI) were defined for the pre-dose (ROI_{pre}) and post-dose (ROI_{post}) data using a correlation coefficient threshold of 0.40 based on the positive BOLD response. A joint functional ROI (ROI_{joint}) was then formed from the intersection of ROI_{pre} and ROI_{post}, using a spatial clustering criterion (one nearest neighbor) to eliminate isolated voxels. The area of the first 2.5 s of the average BOLD response, referred to as the initial dip area, was computed for each voxel within ROI_{joint}, with a negative area corresponding to the presence of an initial dip. Voxels within ROI_{joint} displaying an initial dip in the pre-dose data were then used to define an initial dip ROI, denoted as ROI_{dip}. In other words, ROI_{dip} encompasses all voxels in ROI_{joint} that display an initial dip in the pre-dose periodic BOLD response.

Note that for subjects with both 4-mm and 8-mm slice thickness data, a separate ROI_{dip} was defined for each slice thickness. For each voxel within ROI_{dip}, the average BOLD response was formed by averaging across cycles of the average BOLD time series. For each subject, a mean BOLD response was then computed for ROI_{dip}, and a paired t test (two-tailed) was used to compare the pre-dose and post-dose initial dip areas across all voxels within ROI_{dip}. In addition, the average CBF was computed for ROI_{dip}, and a paired t test (two-tailed) was used to compare the pre-dose and post-dose CBF levels across voxels in ROI_{dip}.

An additional correlation analysis was performed to show localization of the initial dip but was not used for further statistical comparisons. The initial dip reference function was a symmetric triangle that started at 0.5 s, peaked at 1.5 s with a negative amplitude of − 0.5, and returned to zero at 2.5 s (total duration = 2 s). A spatial clustering criterion (one nearest neighbor) was used to eliminate isolated voxels.

Results

The group average pre-dose (blue) and post-dose (red) BOLD responses ($N = 5$) from the 8-mm slice thickness data are shown in the top row of Fig. 1, with panel (b) depicting a magnified view of the initial response. Consistent with prior findings (Liu et al., 2004), the administration of caffeine speeds up the BOLD response with a decrease in peak-time from 8.45 s to 7.45 s and full-width half maximum from 6.95 s to 6.1 s. The peak amplitude increased from 1.83% to 2.16% following caffeine ingestion. In the initial portion of the pre-dose response, the response dips after the onset of the visual stimulus, reaching a minimum value of −0.16% at 1.5 s, at which time the response begins to recover and becomes positive at 2.5 s. In contrast to the pre-dose initial response, the post-dose response increases after the onset of stimulus. Group average responses from the 4-mm slice thickness data ($N = 3$ subjects) are shown in the bottom row of Fig. 1. The results are similar to those observed for the 8-mm slice thickness data, with the initial dip clearly visible in the pre-dose response and reduced in the post-dose response. Following the initial onset of visual stimulation, the pre-dose response dips to a minimum value of −0.24% at 1.5 s before becoming positive at 2.5 s.

Fig. 2 shows the post-dose (y-axis) versus pre-dose (x-axis) initial dip areas from the ROI_{dip} for each subject. Panels a–c and d–h correspond to the data acquired at 4-mm and 8-mm slice thicknesses, respectively. A significant ($P < 8.4e{-}4$) reduction of the initial dip (e.g., more positive initial dip area) was observed for each subject. Fig. 3 shows magnified views of the pre-dose (blue) and post-dose (red) average initial responses for each subject. Panels a–c show the responses from the 4-mm slice thickness data, while panels d–h are for the 8-mm slice thickness data. The reduction of the initial dip by caffeine is clearly present in each subject's responses.

Fig. 4 compares the pre-dose and post-dose spatial localization of the initial dip and the positive BOLD response for a representative slice (4 mm thick) from subject 1. Panels a and c show the spatial extent of the initial dip in the pre-dose and post-dose conditions, respectively, with the colorbar indicating the scale of the correlation coefficient calculated with the initial dip reference function. Consistent with the above observations of a significant reduction of the initial dip with caffeine, the spatial extent of the initial dip is greatly diminished in the post-dose map. Panels b and d are positive BOLD activation maps for the pre-dose and post-dose conditions, respectively, with the colorbar indicating the scale of the correlation coefficients obtained with the positive BOLD reference function. In comparison to the initial dip spatial maps, the positive BOLD maps exhibit a wider spread of activation across the occipital cortex, consistent with the findings of prior studies (Yacoub and Hu, 2001; Yacoub et al., 2001). Spatial localization maps from the other subjects showed similar behavior.

Table 1 shows the average pre-dose and post-dose CBF values for each subject, along with P values obtained with two-tailed paired t tests. The mean and standard deviations of the CBF were

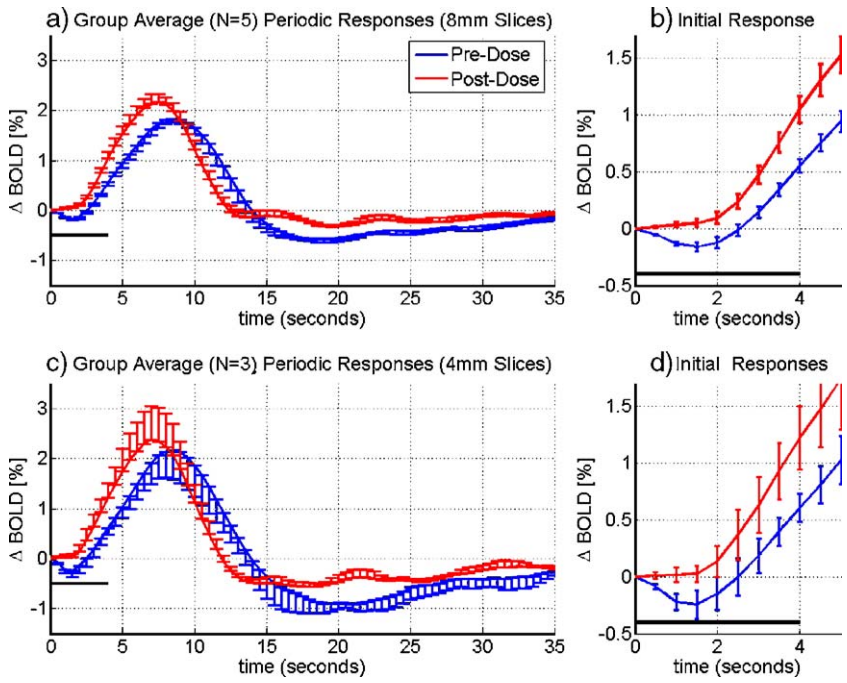

Fig. 1. Pre-dose (blue) and post-dose (red) group averaged periodic BOLD responses acquired with slice thicknesses of 8 mm (a) and 4 mm (c). Averages are from voxels within ROI_{dip} (defined separately for each slice thickness). Magnified views are shown in panels b and d. The initial dip is clearly evident in the pre-dose responses and is absent in the corresponding post-dose responses. The length of each error bar represents the standard error across subjects and the thick black line denotes the stimulus duration. (For interpretation of the references to colour in this figure legend, the reader is referred to the web version of this article.)

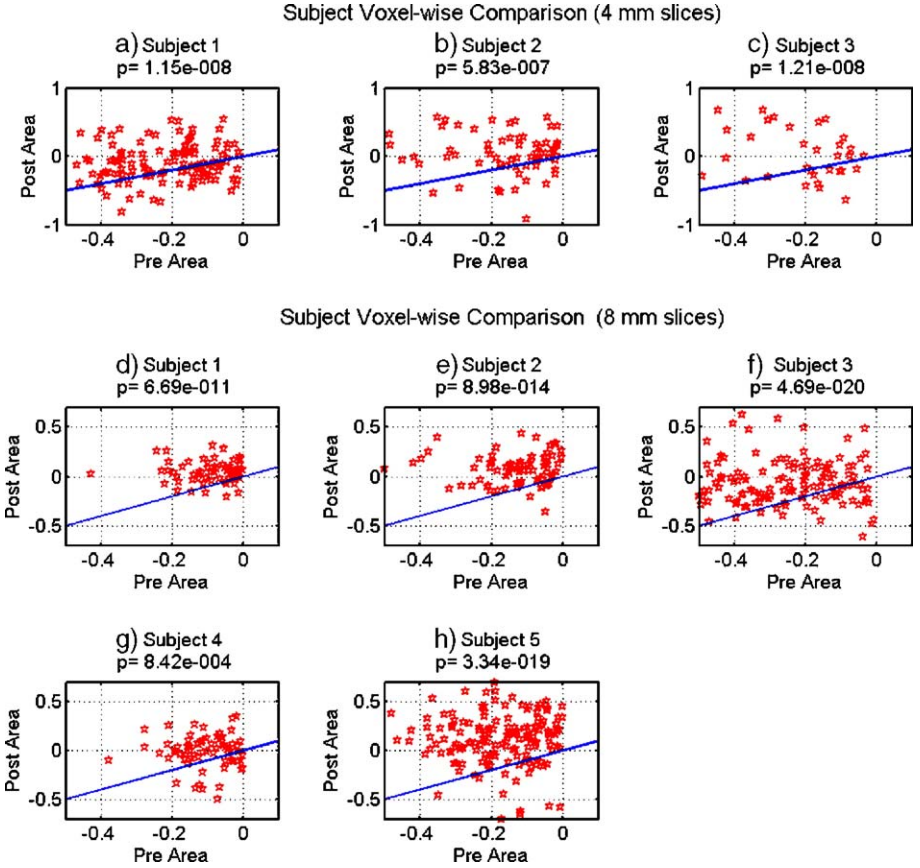

Fig. 2. Comparison of the post-dose (y-axis) and pre-dose (x-axis) initial dip areas for each subject for voxels within ROI_{dip}. The solid line represents the line of equality. Panels a–h represent subject data acquired with slice thicknesses of 4 mm and 8 mm, respectively. The P values were computed with a paired t test (two-tailed).

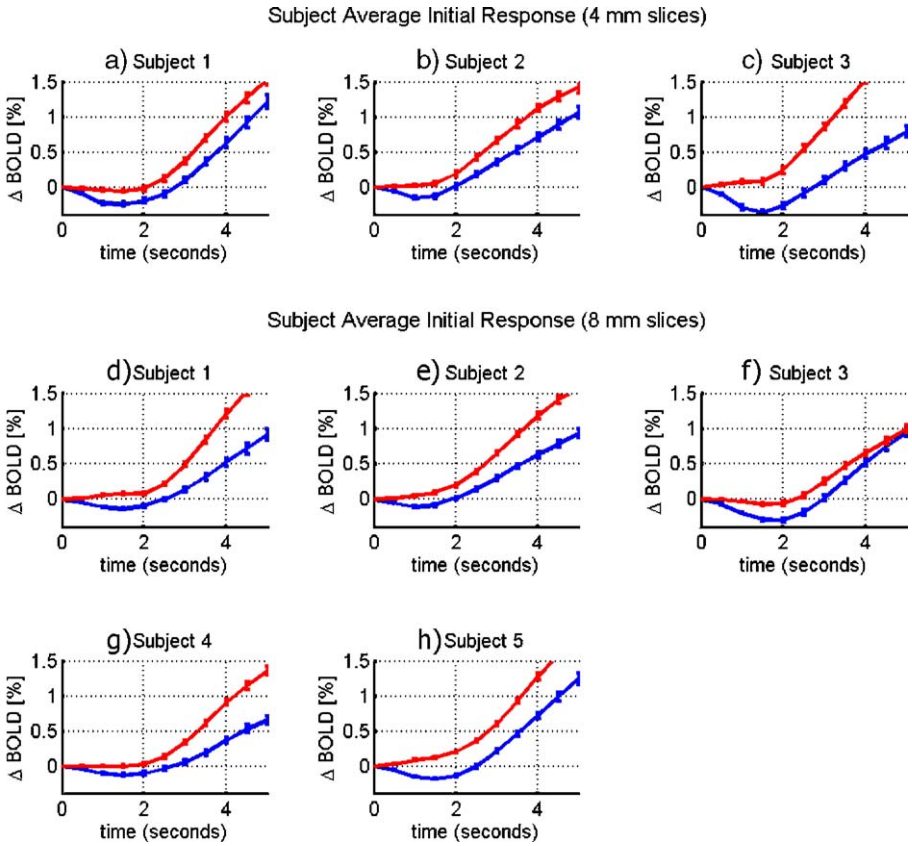

Fig. 3. Magnified views of the pre-dose (blue) and post-dose (red) initial responses for each subject averaged across their respective ROI_{dip}. Panels a–c show the responses from the 4-mm slice thickness data, while panels d–h are for the 8-mm slice thickness data. The error bars represent the standard error across voxels. The reduction of the initial dip by caffeine is clearly present in each subject's responses. (For interpretation of the references to colour in this figure legend, the reader is referred to the web version of this article.)

computed using voxels within each subject's ROI_{dip}. For each subject, there is a significant reduction ($P < 1.7e{-}11$) in CBF associated with the caffeine dose, with the percent decrease in CBF ranging from 30 to 51% across subjects.

Discussion

A significant reduction in the initial dip amplitude due to caffeine was observed in each subject that was studied. This

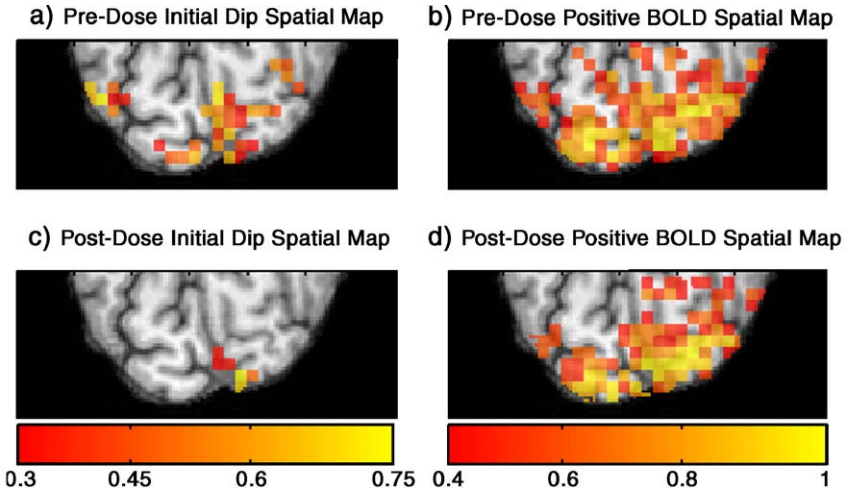

Fig. 4. Comparison of the pre-dose (top row) and post-dose (bottom row) spatial localization maps for the initial dip (left column) and the positive BOLD response (right column) for subject 1. Panels a and c show the spatial extent of the initial dip in the pre-dose and post-dose conditions, respectively, with the colorbar below panel c indicating the scale of the correlation coefficients obtained with the initial dip reference function. Panels b and d are positive BOLD spatial maps for the pre-dose and post-dose conditions, respectively. The colorbar below panel d indicates the scale of the correlation coefficients obtained with the positive BOLD reference function. (For interpretation of the references to colour in this figure legend, the reader is referred to the web version of this article.)

reduction was observed in both 8-mm slice thickness data ($N = 5$) and the 4-mm slice thickness data ($N = 3$), indicating that the effect is fairly robust with respect to voxel size. Consistent with prior studies, the caffeine dose also significantly reduced the baseline CBF level in each subject (Cameron et al., 1990; Field et al., 2003; Liu et al., 2004).

Why does caffeine reduce the initial dip? Caffeine exerts both neural and vascular effects through its binding to adenosine receptors in the brain (Fredholm et al., 1999). In particular, its neurostimulant effects are thought to arise from the inhibition of adenosine A_1 receptors, while its vasoconstrictive effects are believed to be due primarily to the inhibition of adenosine A_{2A} receptors (Ngai et al., 2001). It is reasonable to conjecture that the enhancement of neural activity with caffeine would primarily affect the $CMRO_2$ response, while vasoconstriction due to caffeine is more likely to alter the CBF response. The presence of an initial dip is generally thought to reflect a temporal mismatch between $CMRO_2$ and CBF, with $CMRO_2$ increasingly more rapidly than CBF following the onset of stimulus (Buxton, 2001; Ances, 2004). A reduction in the initial dip could therefore reflect either a relative quickening of the CBF response or a relative slowing down of the $CMRO_2$ response. Given its neurostimulant properties, it seems unlikely that caffeine would cause the $CMRO_2$ response to become slower. In contrast, a quickening of the CBF response due to vasoconstriction would be consistent with the findings of a recent theoretical model introduced by our group (Behzadi and Liu, 2005).

In the theoretical model, the dynamics of the CBF response depend on the biomechanical responsiveness of the arterioles, which in turn depends on the relative contributions of the vascular smooth muscle and connective tissue to the dynamics of the arteriolar wall. With vasodilatory agents, such as carbon dioxide, the vascular smooth muscle relaxes and exerts less force so that the arteriole may expand, while the connective tissue becomes stiffer and exerts more force, similar to the walls of a rubber tube becoming less compliant as it expands. This makes the arteriole relatively less responsive and slows down the dynamic CBF response. In contrast, with the application of a vasoconstrictive agent, such as caffeine, the vascular smooth muscle exerts more force in order to constrict the arteriole, while the force exerted by the connective tissue is reduced. This redistribution of forces makes the arteriole more responsive and speeds up the dynamic CBF response.

While the above arguments suggest that the reduction in the initial dip is due primarily to a quickening of the CBF response, an effect of caffeine on the $CMRO_2$ response cannot be ruled out. It is likely, however, that caffeine-induced changes in the $CMRO_2$ response are smaller than changes in the CBF response. Further experimental studies directly examining the effect of caffeine on the CBF and $CMRO_2$ responses would be useful for clarifying the mechanisms through which caffeine affects the initial dip.

Our finding that caffeine reduces the initial dip in humans may also provide insight into the conflicting reports concerning the initial dip in animals. A number of the studies (Logothetis et al., 1999; Duong et al., 2000; Kim et al., 2000) reporting an initial dip have used isoflurane, which has been shown to increase baseline CBF (Sicard et al., 2003). The isoflurane-induced vasodilation would tend to slow down the CBF response and enhance the initial dip. Recently, Fukuda et al. (2006) showed that the administration of sodium nitroprusside, a vasodilator, significantly attenuated the CBF response to neural stimulus and led to a large and sustained initial dip in cat visual cortex. In contrast, studies using alpha-chloralose, which has been shown to reduce baseline CBF (Nakao et al., 2001), have typically reported an absence of an initial dip, similar to the findings obtained here with caffeine (Mandeville et al., 1999; Marota et al., 1999; Silva et al., 2000). However, as pointed out in Ances (2004), there are counter-examples to these broad trends, such as no initial dip with isoflurane (Lindauer et al., 2001) and an initial dip with alpha-chloralose (Ances et al., 2001). In addition, the initial dip has been observed with urethane, which has been shown to slightly reduce CBF in the hippocampus (Osborne, 1997; Jones et al., 2001). Thus, while the vasoactive properties of anesthesia may account for some of the variability in the animal studies, it is likely that additional factors, such as brain region, animal species, and details of the experimental preparation and imaging method, also play a significant role.

Finally, given the widespread use of dietary caffeine in the general population, it is likely that variability in caffeine usage across subjects plays a significant role in the detection of the initial dip in human fMRI studies, especially in young healthy populations where additional confounding factors such as medication and disease are typically minimal. Caffeine usage should therefore be carefully controlled in human fMRI studies focused on the initial dip.

Acknowledgments

The authors thank Joy Liau for her assistance with the preparation of this paper. This work was supported in part by a grant from the Whitaker Foundation.

References

Ances, B.M., 2004. Coupling of changes in cerebral blood flow with neural activity: what must initially dip must come back up. J. Cereb. Blood Flow Metab. 24 (1), 1–6.

Ances, B.M., Buerk, D.G., Greenberg, J.H., Detre, J.A., 2001. Temporal dynamics of the partial pressure of brain tissue oxygen during functional forepaw stimulation in rats. Neurosci. Lett. 306 (1–2), 106–110.

Behzadi, Y., Liu, T.T., 2005. An arteriolar compliance model of the cerebral blood flow response to neural stimulus. NeuroImage 25 (4), 1100–1111.

Buxton, R.B., 2001. The elusive initial dip. NeuroImage 13 (6 Pt. 1), 953–958.

Buxton, R.B., Wong, E.C., Frank, L.R., 1998. Dynamics of blood flow and oxygenation changes during brain activation: the balloon model. Magn. Reson. Med. 39, 855–864.

Cameron, O.G., Modell, J.G., Hariharan, M., 1990. Caffeine and human cerebral blood flow: a positron emission tomography study. Life Sci. 47 (13), 1141–1146.

Chalela, J., Alsop, D.C., Gonzalez-Atavales, J.B., Maldjian, J.A., Kasner, S.E., Detre, J.A., 2000. Magnetic resonance perfusion imaging in acute ischemic stroke using continuous arterial spin labeling. Stroke 31, 680–687.

Cohen, E.R., Ugurbil, K., Kim, S.G., 2002. Effect of basal conditions on the magnitude and dynamics of the blood oxygenation level-dependent fMRI response. J. Cereb. Blood Flow Metab. 22 (9), 1042–1053.

Cox, R.W., 1996. AFNI-software for analysis and visualization of functional magnetic resonance neuroimages. Comput. Biomed. Res. 29, 162–173.

D'Esposito, M., Deouell, L.Y., Gazzaley, A., 2003. Alterations in the BOLD fMRI signal with ageing and disease: a challenge for neuroimaging. Nat. Rev., Neurosci. 4 (11), 863–872.

Duong, T.Q., Kim, D.S., Ugurbil, K., Kim, S.G., 2000. Spatiotemporal dynamics of the BOLD fMRI signals: toward mapping submillimeter cortical columns using the early negative response. Magn. Reson. Med. 44 (2), 231–242.

Ernst, T., Hennig, J., 1994. Observation of a fast response in functional MR. Magn. Reson. Med. (32), 146–149.

Field, A.S., Laurienti, P.M., Yen, Y.-F., Burdette, J.H., Moody, D.M., 2003. Dietary caffeine consumption and withdrawal: confounding variables in quantitative cerebral perfusion studies? Radiology 227, 129–135.

Fransson, P., Kruger, G., Merboldt, K.D., Frahm, J., 1998. Temporal characteristics of oxygenation-sensitive MRI responses to visual activation in humans. Magn. Reson. Med. 39 (6), 912–919.

Fredholm, B.B., Battig, K., Holmen, J., Nehlig, A., Zvartau, E.E., 1999. Actions of caffeine in the brain with special reference to factors that contribute to its widespread use. Pharmacol. Rev. 51 (1), 83–133.

Fukuda, M., Wang, P., Moon, C., Tanifuji, M., Kim, S.G., 2006. Spatial specificity of the enhanced dip inherently induced by prolonged oxygen consumption in cat visual cortex: implication for columnar resolution functional MRI. NeuroImage 30 (1), 70–87.

Glover, G.H., Li, T.Q., Ress, D., 2000. Image-based method for retrospective correction of physiological motion effects in fMRI: RETROICOR. Magn. Reson. Med. 44 (1), 162–167.

Hu, X., Le, T.H., Ugurbil, K., 1997. Evaluation of the early response in fMRI in individual subjects using short stimulus duration. Magn. Reson. Med. 37, 877–884.

Jones, M., Berwick, J., Johnston, D., Mayhew, J., 2001. Concurrent optical imaging spectroscopy and laser-Doppler flowmetry: the relations hip between blood flow, oxygenation, and volume in rodent barrel cortex. NeuroImage 13 (6 Pt. 1), 1002–1015.

Kemna, L.J., Posse, S., 2001. Effect of respiratory CO(2) changes on the temporal dynamics of the hemodynamic response in functional MR imaging. NeuroImage 14 (3), 642–649.

Kim, D.S., Duong, T.Q., Kim, S.G., 2000. High-resolution mapping of iso-orientation columns by fMRI. Nat. Neurosci. 3 (2), 164–169.

Lindauer, U., Royl, G., Leithner, C., Kuhl, M., Gold, L., Gethmann, J., Kohl-Bareis, M., Villringer, A., Dirnagl, U., 2001. No evidence for early decrease in blood oxygenation in rat whisker cortex in response to functional activation. NeuroImage 13 (6 Pt. 1), 988–1001.

Liu, T.T., Behzadi, Y., Restom, K., Uludag, K., Lu, K., Buracas, G.T., Dubowitz, D.J., Buxton, R.B., 2004. Caffeine alters the temporal dynamics of the visual BOLD response. NeuroImage 23 (4), 1402–1413.

Logothetis, N.K., Guggenberger, H., Peled, S., Pauls, J., 1999. Functional imaging of the monkey brain. Nat. Neurosci. 2 (6), 555–562.

Malonek, D., Grinvald, A., 1996. Interactions between electrical activity and cortical microcirculation revealed by imaging spectroscopy: implications for functional brain mapping. Science 272, 551–554.

Mandeville, J.B., Marota, J.J., Ayata, C., Moskowitz, M.A., Weisskoff, R.M., Rosen, B.R., 1999. MRI measurement of the temporal evolution of relative CMRO(2) during rat forepaw stimulation. Magn. Reson. Med. 42 (5), 944–951.

Marota, J.J., Ayata, C., Moskowitz, M.A., Weisskoff, R.M., Rosen, B.R., Mandeville, J.B., 1999. Investigation of the early response to rat forepaw stimulation. Magn. Reson. Med. 41 (2), 247–252.

Menon, R.S., Ogawa, S., Strupp, J.P., Anderson, P., Ugurbil, K., 1995. BOLD based functional MRI at 4 Tesla includes a capillary bed contribution: echo-planar imaging correlates with previous optical imaging using intrinsic signals. Magn. Reson. Med. 33, 453–459.

Nakao, Y., Itoh, Y., Kuang, T.Y., Cook, M., Jehle, J., Sokoloff, L., 2001. Effects of anesthesia on functional activation of cerebral blood flow and metabolism. Proc. Natl. Acad. Sci. U. S. A. 98 (13), 7593–7598.

Ngai, A.C., Coyne, E.F., Meno, J.R., West, G.A., Winn, H.R., 2001. Receptor subtypes mediating adenosine-induced dilation of cerebral arterioles. Am. J. Physiol., Heart Circ. Physiol. 280 (5), H2329–H2335.

Osborne, P.G., 1997. Hippocampal and striatal blood flow during behavior in rats: chronic laser Doppler flowmetry study. Physiol. Behav. 61 (4), 485–492.

Restom, K., Behzadi, Y., Uludag, K., Liu, T.T., 2004. Image based physiological noise correction for perfusion-based fMRI. Proceedings of the 12th ISMRM Scientific Meeting, Kyoto, pp. 2525.

Sicard, K., Shen, Q., Brevard, M.E., Sullivan, R., Ferris, C.F., King, J.A., Duong, T.Q., 2003. Regional cerebral blood flow and BOLD responses in conscious and anesthetized rats under basal and hypercapnic conditions: implications for functional MRI studies. J. Cereb. Blood Flow Metab. 23 (4), 472–481.

Silva, A.C., Lee, S.P., Iadecola, C., Kim, S.G., 2000. Early temporal characteristics of cerebral blood flow and deoxyhemoglobin changes during somatosensory stimulation. J. Cereb. Blood Flow Metab. 20 (1), 201–206.

Thompson, J.K., Peterson, M.R., Freeman, R.D., 2004. High-resolution neurometabolic coupling revealed by focal activation of visual neurons. Nat. Neurosci. 7 (9), 919–920.

Vanzetta, I., Grinvald, A., 1999. Increased cortical oxidative metabolism due to sensory stimulation: implications for functional brain imaging. Science 286 (5444), 1555–1558.

Wang, J., Qiu, M., Constable, R.T., 2005. In vivo method for correcting transmit/receive nonuniformities with phased array coils. Magn. Reson. Imaging 53, 666–674.

Wong, E.C., Buxton, R.B., Frank, L.R., 1998. Quantitative imaging of perfusion using a single subtraction (QUIPSS and QUIPSS II). Magn. Reson. Med. 39 (5), 702–708.

Yacoub, E., Hu, X., 2001. Detection of the early decrease in fMRI signal in the motor area. Magn. Reson. Med. 45 (2), 184–190.

Yacoub, E., Le, T.H., Ugurbil, K., Hu, X., 1999. Further evaluation of the initial negative response in functional magnetic resonance imaging. Magn. Reson. Med. 41 (3), 436–441.

Yacoub, E., Shmuel, A., Pfeuffer, J., Van De Moortele, P.F., Adriany, G., Ugurbil, K., Hu, X., 2001. Investigation of the initial dip in fMRI at 7 Tesla. NMR Biomed. 14 (7–8), 408–412.